Acta Cryst E CRYSTALLOGRAPHIC COMMUNICATIONS

ISSN 2056-9890

Synthesis and crystal structure of $NaCuIn(PO_4)_2$

Elhassan Benhsina,[a]* Jamal Khmiyas,[a] Said Ouaatta,[a] Abderrazzak Assani,[b] Mohamed Saadi[b] and Lahcen El Ammari[b]

[a]Laboratoire de Chimie Appliquée des Matériaux, Centre des Sciences des Matériaux, Faculty of Sciences, Mohammed V University in Rabat, Avenue Ibn Batouta, BP 1014, Rabat, Morocco, and [b]Laboratoire de Chimie Appliquée des Matériaux, Centre des Sciences des Matériaux, Faculty of Sciences, Mohammed V University in Rabat, Avenue Ibn Batouta, B.P. 1014, Rabat, Morocco. *Correspondence e-mail: el_benhsina@yahoo.fr

Received 20 January 2020
Accepted 10 February 2020

Edited by M. Weil, Vienna University of Technology, Austria

Keywords: crystal structure; phosphate; $AMM'(PO_4)_2$ family; trigonal–bipyramidal coordination; isotypism.

CCDC reference: 1983244

Supporting information: this article has supporting information at journals.iucr.org/e

Single crystals of sodium copper(II) indium bis[phosphate(V)], $NaCuIn(PO_4)_2$, were grown from the melt under atmospheric conditions. The title phosphate crystallizes in the space group $P2_1/n$ and is isotypic with $KCuFe(PO_4)_2$. In the crystal, two $[CuO_5]$ trigonal bipyramids share an edge to form a dimer $[Cu_2O_8]$ that is connected to two PO_4 tetrahedra. The obtained $[Cu_2P_2O_{12}]$ units are interconnected through vertices to form sheets that are sandwiched between undulating layers resulting from the junction of PO_4 tetrahedra and $[InO_6]$ octahedra. The two types of layers are alternately stacked along [101] and are joined into a three-dimensional framework through vertex- and edge-sharing, leaving channels parallel to the stacking direction. The channels host the sodium cations that are surrounded by four oxygen atoms in form of a distorted disphenoid.

1. Chemical context

Transition-metal phosphates have been the subject of intensive research as a result of their interesting physical properties and potential applications in wide-ranging fields such as catalysis, electrochemistry, luminescence (Tie *et al.*, 1995; Pan *et al.*, 2006; Yang *et al.*, 2016) and ion exchange (Cheetham *et al.*, 1999; Han *et al.*, 2015; Manos *et al.*, 2005, 2007; Plabst *et al.*, 2009; Stadie *et al.*, 2017). In these materials, the anionic framework is built up from PO_4 tetrahedra linked to different kinds of transition metal (*TM*) coordination polyhedra of the form $[TMO_n]$ (n = 4, 5 and 6), leading to a large variety of crystal structure families. This structural diversity is mainly associated with the ability of *TM* cations to adopt different oxidation states in various coordination polyhedra. Based on previous hydrothermal investigations aimed at orthophosphates of general formula $(M,M'')_3(PO_4)_2{\cdot}nH_2O$ (M and M'' = bivalent cations), we have reported on synthesis and characterization of the phosphates $Ni_2Sr(PO_4)_2{\cdot}2H_2O$ (Assani *et al.*, 2010), $Mg_{1.65}Cu_{1.35}(PO_4)_2{\cdot}H_2O$ (Khmiyas *et al.*, 2015) and $Mn_2Zn(PO_4)_2{\cdot}H_2O$ (Alhakmi *et al.*, 2015). In this context, the aim of the present study was to develop new phases belonging to the series $AM''M'''(PO_4)_2$ where A, M'' and M''' are mono-, bi- and trivalent cations, respectively. As a result, we report here on synthesis and crystal structure of the new compound $NaCuIn(PO_4)_2$.

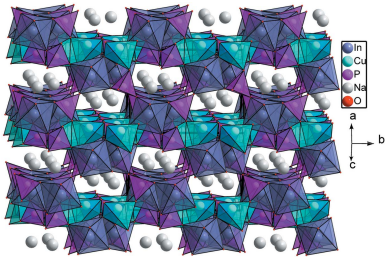

2. Structural commentary

The principal building units of the crystal structure of $NaCuIn(PO_4)_2$ are two PO_4 tetrahedra linked to a $[CuO_5]$

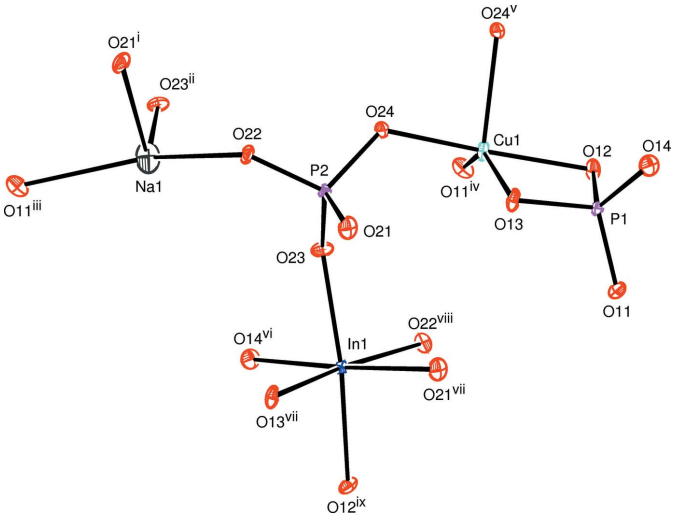

Figure 1
The principal building units in the crystal structure of $NaCuIn(PO_4)_2$. Displacement ellipsoids are drawn at the 50% probability level. [Symmetry codes: (i) $x+\frac{1}{2}, -y-\frac{1}{2}, z+\frac{1}{2}$; (ii) $-x+1, -y, -z+2$; (iii) $-x+\frac{1}{2}, y-\frac{1}{2}, -z+\frac{3}{2}$; (iv) $x+\frac{1}{2}, -y+\frac{1}{2}, z+\frac{1}{2}$; (v) $-x+1, -y, -z+1$; (vi) $x, y, z+1$; (vii) $-x, -y, -z+1$; (viii) $-x+\frac{1}{2}, y+\frac{1}{2}, -z+\frac{3}{2}$; (ix) $x-\frac{1}{2}, -y+\frac{1}{2}, z+\frac{1}{2}$.]

triangular bipyramid [Cu—O bond-length range of 1.9088 (9) to 2.1939 (9) Å] and to an [InO_6] octahedron [In—O bond lengths range from 2.1028 (10) to 2.2051 (9) Å], and is completed by a distorted [NaO_4] polyhedron (Fig. 1). The P—O bond lengths in the two phosphate tetrahedra are similar and comparable with those of similar phosphates. However, the P1—O distances, varying between 1.5035 (10) and 1.5729 (9) Å, indicate a somewhat higher distortion of this tetrahedron than the P2—O distances [between 1.5297 (9) and 1.5488 (9) Å] of the other tetrahedron.

In this phosphate, two [CuO_5] triangular bipyramids share one edge to form a [Cu_2O_8] dimer, the ends of which are linked to two $P1O_4$ tetrahedra by edge-sharing. The obtained [$Cu_2P_2O_{12}$] groups are linked together *via* the vertices to form sheets extending parallel to $(10\bar{1})$, as shown in Fig. 2. On the other hand, the [InO_6] octahedra and the $P2O_4$ tetrahedra are interconnected through common vertices to build up an undulating layer extending in the same direction (Fig. 3). The copper phosphate layers are sandwiched between the undulating indium phosphate layers. By sharing corners and edges, an alternating stacking of the layers along [101] leads to a three-dimensional framework structure with channels in which the Na^+ cations are located (Fig. 4). The four nearest oxygen atoms around the alkali metal cation form a distorted disphenoid with Na—O distances between 2.3213 (12) and 2.4275 (11) Å (Fig. 1).

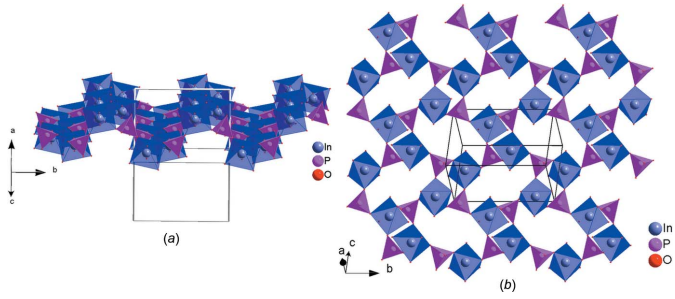

Figure 3
(*a*) A view approximately along [101] showing the undulating layer formed by [InO_6] octahedra linked to PO_4 tetrahedra and (*b*) a projection of this layer onto (101).

$NaCuIn(PO_4)_2$ is isotypic with $KCuFe(PO_4)_2$ (Badri *et al.*, 2011), whereby potassium is substituted by sodium and iron by indium. However, we note a significant difference in the coordination number of sodium and potassium in the two structures. Whereas sodium has a fourfold coordination in $NaCuIn(PO_4)_2$, potassium is surrounded by nine oxygen atoms in $KCuFe(PO_4)_2$ because of its greater ionic radius.

Bond-valence-sum calculations (Brown & Altermatt, 1985) are in good agreement with the expected values (in valence units) for sodium(I), copper(II), indium(III) and the phosphorus(V) cations, *viz*. $Na^I = 0.845$ (2), $Cu^{II} = 2.102$ (3), $In^{III} = 3.152$ (4), $P1^V = 4.930$ (8), and $P2^V = 4.992$ (8). For the

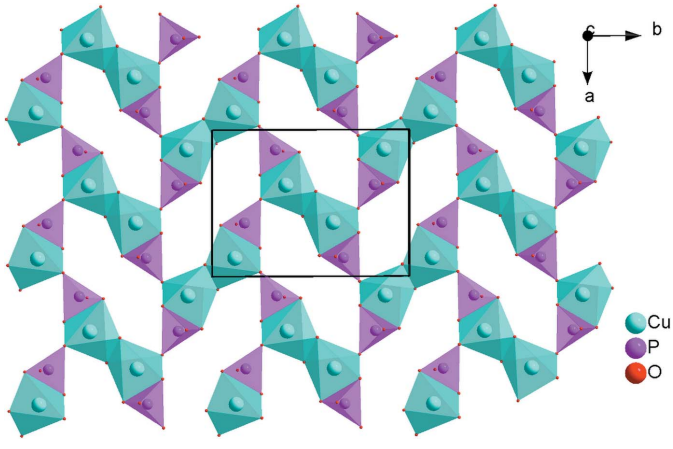

Figure 2
Projection along [001] of [$Cu_2P_2O_{12}$] copper phosphate sheets in the crystal structure of $NaCuIn(PO_4)_2$.

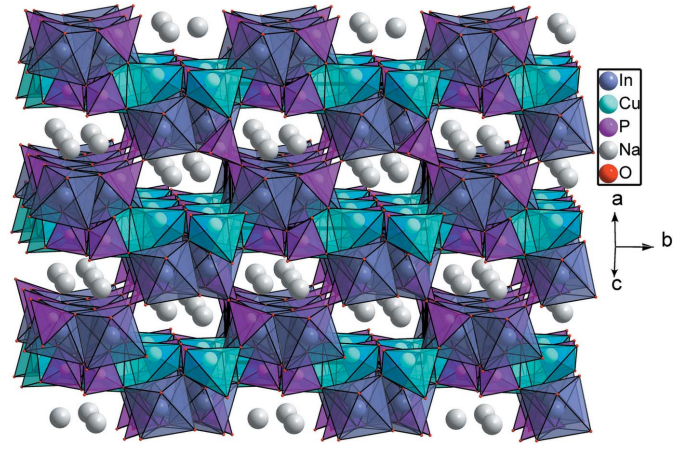

Figure 4
The sodium cations located in channels running parallel to [101] in the crystal structure of $NaCuIn(PO_4)_2$.

oxygen anions, the calculated values range between 1.940 (5) and 2.076 (3).

3. Database survey

Phosphate-based materials with general formula $AM^{II}M'^{III}(PO_4)_2$ commonly show crystal structures where channels or, more rarely, layers are formed by the $[M^{II}M'^{II}(PO_4)_2]^-$ framework to delimit suitable environments to accommodate the A^+ cations. A recent survey given by Yakubovich *et al.* (2019) revealed that all compounds of the morphotropic series $AM^{II}M'^{III}(PO_4)_2$, where A = Na, K, Rb or NH_4, M'' = Cu, Ni, Co, Fe, Zn or Mg and M''' = Fe, Al or Ga, crystallize in the monoclinic crystal system and can be classified into seven subgroups according to their structure types, *viz*. (i) $KNiFe(PO_4)_2$ (space-group type $P2_1/c$, Z = 4; Strutynska *et al.*, 2014); (ii) $KFe^{II}Fe^{III}(PO_4)_2$ (space-group type $P2_1/c$, Z = 4; Yakubovich *et al.*, 1986); (iii) $(NH_4)Fe^{II}Fe^{III}(PO_4)_2$ (space-group type $C2/c$, Z =16; Boudin & Lii, 1998); (iv) $K(Co,Al)_2(PO_4)_2$ (space-group type $C2/c$, Z = 8; Chen *et al.*, 1997); (v) $(NH_4)(Zn,Ga)_2(PO_4)_2$ (space-group type $P2_1/a$, Z = 4; Logar *et al.*, 2001); (vi) $KMgFe(PO_4)_2$ (space-group type $C2/c$, Z = 4; Badri *et al.*, 2009); (vii) $NaZnAl(PO_4)_2$ (space-group type $P2_1/c$, Z = 4; Yakubovich *et al.*, 2019). $NaCuIn(PO_4)_2$ belongs to the second subgroup of this classification.

In addition, the structures of certain members of this phosphate family are similar to those of the zeolite-*AB*W structural type (Badri *et al.*, 2014). When the trivalent cation is lanthanum or yttrium, the crystal structures $KM^{II}La(PO_4)_2$ (M^{II} = Mg or Zn) are isotypes of the monazite monoclinic structure of $LaPO_4$ with space-group type $P2_1/n$ (Pan *et al.*, 2006; Tie *et al.*, 1995), while $KMgY(PO_4)_2$ turns out to be an isotype of the xenotime structure YPO_4 adopting a tetragonal symmetry with space-group type $I4_1/amd$ (Tie *et al.*, 1996).

4. Synthesis and crystallization

Stoichiometric amounts of $NaNO_3$, CuO, In_2O_3 and $NH_4H_2PO_4$ as precursors in the molar ratio 1:1:0.5:2 were ground in an agate mortar and pre-heated at 473 and 673 K in a platinum crucible to eliminate gaseous products. The resulting powder was subsequently heated to a temperature of 1473 K. The product was then cooled to room temperature at a rate of 5 K h^{-1}. The obtained product contained green single crystals corresponding to the title phosphate.

5. Refinement

Crystal data, data collection and structure refinement details are summarized in Table 1.

Labelling of atoms and their coordinates were adapted from isotypic $KCuFe(PO_4)_2$ (Badri *et al.*, 2011). Since not all atoms in the latter description are part of one unit cell, a translation by (z + 1) relative to the original coordinates brings all corresponding atoms inside one unit cell. Moreover, oxygen atoms O11 and O14 were translated by $(x-\frac{1}{2}, -y+\frac{1}{2}, z-\frac{1}{2})$ and $(x, y, z-1)$, respectively, to be linked directly to P1.

The maximum and minimum electron densities in the final difference-Fourier map are at 0.70 Å from O14 and 0.50 Å from Cu1, respectively.

Table 1
Experimental details.

Crystal data	
Chemical formula	$NaCuIn(PO_4)_2$
M_r	391.29
Crystal system, space group	Monoclinic, $P2_1/n$
Temperature (K)	296
a, b, c (Å)	8.2563 (3), 10.1382 (4), 8.8060 (3)
β (°)	114.444 (1)
V (Å^3)	671.03 (4)
Z	4
Radiation type	Mo $K\alpha$
μ (mm^{-1})	7.16
Crystal size (mm)	0.34 × 0.25 × 0.19
Data collection	
Diffractometer	Bruker X8 *APEX* Diffractometer
Absorption correction	Multi-scan (*SADABS*; Krause *et al.*, 2015)
T_{min}, T_{max}	0.528, 0.747
No. of measured, independent and observed [$I > 2\sigma(I)$] reflections	24292, 3106, 2996
R_{int}	0.026
(sin $\theta/\lambda)_{max}$ (Å^{-1})	0.820
Refinement	
$R[F^2 > 2\sigma(F^2)]$, $wR(F^2)$, S	0.013, 0.033, 1.11
No. of reflections	3106
No. of parameters	119
$\Delta\rho_{max}$, $\Delta\rho_{min}$ (e Å^{-3})	0.66, −0.59

Computer programs: *APEX2* and *SAINT* (Bruker, 2009), *SHELXT2014/5* (Sheldrick, 2015*a*), *SHELXL2018/3* (Sheldrick, 2015*b*), *ORTEP-3 for Windows* (Farrugia, 2012), *DIAMOND* (Brandenburg, 2006) and *publCIF* (Westrip, 2010).

Acknowledgements

The authors thank the Unit of Support for Technical and Scientific Research (UATRS, CNRST) for the X-ray measurements.

Funding information

Mohammed V University, Rabat, Morocco, is thanked for financial support.

References

Alhakmi, G., Assani, A., Saadi, M. & El Ammari, L. (2015). *Acta Cryst.* E**71**, 154–156.
Assani, A., Saadi, M., Zriouil, M. & El Ammari, L. (2010). *Acta Cryst.* E**66**, i86–i87.
Badri, A., Hidouri, M., López, M. L., Pico, C., Wattiaux, A. & Amara, M. B. (2011). *J. Solid State Chem.* **184**, 937–944.
Badri, A., Hidouri, M., López, M. L., Veiga, M. L., Wattiaux, A. & Amara, M. B. (2009). *Solid State Ionics*, **180**, 1558–1563.
Badri, A., Hidouri, M., Wattiaux, A., López, M. L., Veiga, M. L. & Amara, M. B. (2014). *Mater. Res. Bull.* **55**, 61–66.
Boudin, S. & Lii, K.-H. (1998). *Inorg. Chem.* **37**, 799–803.
Brandenburg, K. (2006). *DIAMOND*. Crystal Impact GbR, Bonn, Germany.
Brown, I. D. & Altermatt, D. (1985). *Acta Cryst.* B**41**, 244–247.

Bruker (2009). *APEX2* and *SAINT*. Bruker AXS Inc., Madison, Wisconsin, USA.
Cheetham, A. K., Férey, G. & Loiseau, T. (1999). *Angew. Chem. Int. Ed.* **38**, 3268–3292.
Chen, X.-A., Zhao, L., Li, Y., Guo, F. & Chen, B.-M. (1997). *Acta Cryst.* C**53**, 1754–1756.
Farrugia, L. J. (2012). *J. Appl. Cryst.* **45**, 849–854.
Han, M. H., Gonzalo, E., Singh, G. & Rojo, T. (2015). *Energy Environ. Sci.* **8**, 81–102.
Khmiyas, J., Assani, A., Saadi, M. & El Ammari, L. (2015). *Acta Cryst.* E**71**, 55–57.
Krause, L., Herbst-Irmer, R., Sheldrick, G. M. & Stalke, D. (2015). *J. Appl. Cryst.* **48**, 3–10.
Logar, N. Z., Mrak, M., Kaučič, V. & Golobič, A. (2001). *J. Solid State Chem.* **156**, 480–486.
Manos, M. J., Iyer, R. G., Quarez, E., Liao, J. H. & Kanatzidis, M. G. (2005). *Angew. Chem. Int. Ed.* **44**, 3552–3555.
Manos, M. J., Malliakas, C. D. & Kanatzidis, M. G. (2007). *Chem. Eur. J.* **13**, 51–58.
Pan, Y., Zhang, Q. & Jiang, Z. (2006). *Mater. Sci. Eng. B*, **133**, 186–190.
Plabst, M., McCusker, L. B. & Bein, T. (2009). *J. Am. Chem. Soc.* **131**, 18112–18118.
Sheldrick, G. M. (2015*a*). *Acta Cryst.* C**71**, 3–8.
Sheldrick, G. M. (2015*b*). *Acta Cryst.* A**71**, 3–8.
Stadie, N. P., Wang, S., Kravchyk, K. V. & Kovalenko, M. V. (2017). *ACS Nano*, **11**, 1911–1919.
Strutynska, N. Yu., Zatovsky, I. V., Baumer, V. N., Ogorodnyk, I. V. & Slobodyanik, N. S. (2014). *Acta Cryst.* C**70**, 160–164.
Tie, S., Su, Q. & Yu, Y. (1995). *Phys. Status Solidi A*, **147**, 267–276.
Tie, S., Su, Q., Yu, Y. & Ma, J. (1996). *Chin. J. Chem.* **14**, 25–30.
Westrip, S. P. (2010). *J. Appl. Cryst.* **43**, 920–925.
Yakubovich, O., Kiriukhina, G., Volkov, A. & Dimitrova, O. (2019). *Acta Cryst.* C**75**, 514–522.
Yakubovich, O. V., Evdokimova, O. A., Mel'nikov, O. K. & Simonov, M. A. (1986). *Kristallografiya*, **31**, 906–912.
Yang, Z., Bai, Q., Li, T., Xu, S., Dong, H., Wang, Z. & Li, P. (2016). *Optik*, **127**, 9338–9343.

supporting information

Acta Cryst. (2020). E**76**, 366-369 [https://doi.org/10.1107/S2056989020001929]

Synthesis and crystal structure of $NaCuIn(PO_4)_2$

Elhassan Benhsina, Jamal Khmiyas, Said Ouaatta, Abderrazzak Assani, Mohamed Saadi and Lahcen El Ammari

Computing details

Data collection: *APEX2* (Bruker, 2009); cell refinement: *SAINT* (Bruker, 2009); data reduction: *SAINT* (Bruker, 2009); program(s) used to solve structure: *SHELXT2014/5* (Sheldrick, 2015a); program(s) used to refine structure: *SHELXL2018/3* (Sheldrick, 2015b); molecular graphics: *ORTEP-3 for Windows* (Farrugia, 2012), *DIAMOND* (Brandenburg, 2006); software used to prepare material for publication: *publCIF* (Westrip, 2010).

Sodium copper(II) indium bis[phosphate(V)]

Crystal data

$NaCuIn(PO_4)_2$
M_r = 391.29
Monoclinic, $P2_1/n$
a = 8.2563 (3) Å
b = 10.1382 (4) Å
c = 8.8060 (3) Å
β = 114.444 (1)°
V = 671.03 (4) Å^3
Z = 4
$F(000)$ = 732
D_x = 3.873 Mg m^{-3}
Mo $K\alpha$ radiation, λ = 0.71073 Å
Cell parameters from 3106 reflections
θ = 2.9–35.6°
μ = 7.16 mm^{-1}
T = 296 K
Block, green
0.34 × 0.25 × 0.19 mm

Data collection

Bruker X8 APEX Diffractometer
Radiation source: fine-focus sealed tube
Graphite monochromator
φ and ω scans
Absorption correction: multi-scan (SADABS; Krause *et al.*, 2015)
T_{min} = 0.528, T_{max} = 0.747
24292 measured reflections
3106 independent reflections
2996 reflections with $I > 2\sigma(I)$
R_{int} = 0.026
θ_{max} = 35.6°, θ_{min} = 2.9°
h = −12→13
k = −16→16
l = −14→14

Refinement

Refinement on F^2
Least-squares matrix: full
$R[F^2 > 2\sigma(F^2)]$ = 0.013
$wR(F^2)$ = 0.033
S = 1.11
3106 reflections
119 parameters
0 restraints
$w = 1/[\sigma^2(F_o^2) + (0.0139P)^2 + 0.5758P]$ where $P = (F_o^2 + 2F_c^2)/3$
$(\Delta/\sigma)_{max}$ = 0.004
$\Delta\rho_{max}$ = 0.66 e Å^{-3}
$\Delta\rho_{min}$ = −0.59 e Å^{-3}
Extinction correction: SHELXL-2018/3 (Sheldrick, 2015b), $Fc^*=kFc[1+0.001xFc^2\lambda^3/\sin(2\theta)]^{-1/4}$
Extinction coefficient: 0.0093 (3)

Special details

Geometry. All esds (except the esd in the dihedral angle between two l.s. planes) are estimated using the full covariance matrix. The cell esds are taken into account individually in the estimation of esds in distances, angles and torsion angles; correlations between esds in cell parameters are only used when they are defined by crystal symmetry. An approximate (isotropic) treatment of cell esds is used for estimating esds involving l.s. planes.

Fractional atomic coordinates and isotropic or equivalent isotropic displacement parameters (Å²)

	x	*y*	*z*	U_{iso}*/U_{eq}
Na1	0.51418 (10)	−0.16856 (7)	1.09748 (8)	0.01965 (13)
Cu1	0.37225 (2)	0.11940 (2)	0.45881 (2)	0.00706 (3)
In1	0.00214 (2)	0.12812 (2)	0.73403 (2)	0.00463 (3)
P1	0.12997 (4)	0.17027 (3)	0.15664 (4)	0.00494 (5)
O11	−0.03216 (13)	0.25215 (10)	0.13588 (12)	0.01037 (15)
O12	0.30223 (12)	0.24790 (9)	0.27141 (11)	0.00812 (14)
O13	0.14612 (12)	0.04925 (9)	0.27222 (11)	0.00824 (14)
O14	0.13759 (14)	0.12965 (10)	−0.00448 (12)	0.01159 (16)
P2	0.28460 (4)	−0.08358 (3)	0.66933 (4)	0.00448 (5)
O21	0.11495 (13)	−0.13653 (9)	0.52826 (12)	0.00993 (15)
O22	0.37706 (12)	−0.19241 (8)	0.79630 (11)	0.00787 (14)
O23	0.24068 (13)	0.03111 (9)	0.75876 (12)	0.00903 (15)
O24	0.41607 (13)	−0.03247 (9)	0.59836 (12)	0.00962 (15)

Atomic displacement parameters (Å²)

	U^{11}	U^{22}	U^{33}	U^{12}	U^{13}	U^{23}
Na1	0.0288 (3)	0.0145 (3)	0.0146 (3)	−0.0042 (2)	0.0079 (3)	−0.0035 (2)
Cu1	0.00887 (7)	0.00557 (6)	0.00492 (6)	−0.00104 (4)	0.00104 (5)	0.00126 (4)
In1	0.00517 (4)	0.00405 (4)	0.00432 (4)	−0.00022 (2)	0.00161 (3)	−0.00042 (2)
P1	0.00552 (11)	0.00490 (11)	0.00367 (11)	−0.00020 (9)	0.00119 (9)	0.00053 (8)
O11	0.0096 (4)	0.0125 (4)	0.0094 (4)	0.0054 (3)	0.0044 (3)	0.0042 (3)
O12	0.0085 (4)	0.0077 (3)	0.0063 (3)	−0.0034 (3)	0.0012 (3)	0.0008 (3)
O13	0.0091 (4)	0.0055 (3)	0.0071 (3)	−0.0028 (3)	0.0004 (3)	0.0020 (3)
O14	0.0129 (4)	0.0165 (4)	0.0043 (3)	0.0025 (3)	0.0025 (3)	−0.0014 (3)
P2	0.00536 (11)	0.00392 (11)	0.00410 (11)	0.00089 (8)	0.00189 (9)	0.00025 (8)
O21	0.0096 (4)	0.0119 (4)	0.0054 (3)	−0.0026 (3)	0.0002 (3)	−0.0013 (3)
O22	0.0109 (4)	0.0058 (3)	0.0073 (3)	0.0032 (3)	0.0041 (3)	0.0027 (3)
O23	0.0088 (4)	0.0071 (3)	0.0113 (4)	0.0018 (3)	0.0042 (3)	−0.0034 (3)
O24	0.0101 (4)	0.0092 (4)	0.0125 (4)	0.0030 (3)	0.0077 (3)	0.0056 (3)

Geometric parameters (Å, º)

Na1—O21^{i}	2.3213 (12)	In1—O22^{viii}	2.1441 (9)
Na1—O23^{ii}	2.3496 (12)	In1—O13^{vii}	2.1632 (9)
Na1—O22	2.4268 (11)	In1—O12^{ix}	2.2051 (9)
Na1—O11^{iii}	2.4275 (11)	P1—O14	1.5035 (10)
Cu1—O24	1.9088 (9)	P1—O11	1.5205 (10)
Cu1—O11^{iv}	1.9317 (9)	P1—O13	1.5642 (9)

Cu1—O12	1.9913 (9)	P1—O12	1.5729 (9)
Cu1—O13	2.0378 (9)	P2—O23	1.5297 (9)
Cu1—O24^{v}	2.1939 (9)	P2—O22	1.5310 (9)
In1—O14^{vi}	2.1028 (10)	P2—O21	1.5340 (10)
In1—O21^{vii}	2.1044 (9)	P2—O24	1.5488 (9)
In1—O23	2.1303 (9)		

O21^{i}—Na1—O23^{ii}	108.90 (4)	O14^{vi}—In1—O13^{vii}	94.18 (4)
O21^{i}—Na1—O22	71.58 (4)	O21^{vii}—In1—O13^{vii}	90.44 (4)
O23^{ii}—Na1—O22	123.80 (4)	O23—In1—O13^{vii}	96.21 (4)
O21^{i}—Na1—O11^{iii}	94.99 (4)	O22^{viii}—In1—O13^{vii}	171.80 (3)
O23^{ii}—Na1—O11^{iii}	88.91 (4)	O14^{vi}—In1—O12^{ix}	85.65 (4)
O22—Na1—O11^{iii}	146.95 (4)	O21^{vii}—In1—O12^{ix}	96.23 (4)
O24—Cu1—O11^{iv}	96.82 (4)	O23—In1—O12^{ix}	164.87 (3)
O24—Cu1—O12	166.88 (4)	O22^{viii}—In1—O12^{ix}	87.16 (3)
O11^{iv}—Cu1—O12	96.28 (4)	O13^{vii}—In1—O12^{ix}	91.55 (3)
O24—Cu1—O13	95.96 (4)	O14—P1—O11	114.50 (6)
O11^{iv}—Cu1—O13	144.90 (4)	O14—P1—O13	111.94 (5)
O12—Cu1—O13	72.85 (3)	O11—P1—O13	109.89 (5)
O24—Cu1—O24^{v}	82.35 (4)	O14—P1—O12	111.32 (5)
O11^{iv}—Cu1—O24^{v}	110.97 (4)	O11—P1—O12	108.72 (5)
O12—Cu1—O24^{v}	93.34 (4)	O13—P1—O12	99.40 (5)
O13—Cu1—O24^{v}	103.05 (4)	O23—P2—O22	108.94 (5)
O14^{vi}—In1—O21^{vii}	174.97 (4)	O23—P2—O21	110.57 (5)
O14^{vi}—In1—O23	80.87 (4)	O22—P2—O21	110.58 (5)
O21^{vii}—In1—O23	96.68 (4)	O23—P2—O24	107.97 (5)
O14^{vi}—In1—O22^{viii}	93.79 (4)	O22—P2—O24	108.36 (5)
O21^{vii}—In1—O22^{viii}	81.66 (3)	O21—P2—O24	110.35 (5)
O23—In1—O22^{viii}	86.94 (4)		

Symmetry codes: (i) $x+1/2, -y-1/2, z+1/2$; (ii) $-x+1, -y, -z+2$; (iii) $-x+1/2, y-1/2, -z+3/2$; (iv) $x+1/2, -y+1/2, z+1/2$; (v) $-x+1, -y, -z+1$; (vi) $x, y, z+1$; (vii) $-x, -y, -z+1$; (viii) $-x+1/2, y+1/2, -z+3/2$; (ix) $x-1/2, -y+1/2, z+1/2$.